Journal of the Faculty of Environmental Science and Technology, Okayama University
Vol.3, No.1, pp.75-95, January 1998

Wave-Induced Pore-Pressure Response on a Submarine Pipeline Buried in Seabed Sediments — Experiment and Numerical Verification —

Waldemar MAGDA *, Shiro MAENO ** and Hiroshi NAGO **

(Received October 31 , 1997)

The response of sandy seabed sediments to a harmonically oscillating water-table, with a special consideration of the wave-induced pore-pressure oscillations around a pipeline buried in seabed sediments, is studied in the present work experimentally and numerically. The aim of the analysis was: (1) to observe a true distribution pattern of the wave-induced pore-pressure oscillations acting on the pipeline outer surface, and (2) to verify small-scale test results using numerical computations performed for a wide range of saturation conditions of seabed sediments, under the assumption of a compressible two-phase medium compound of the pore-fluid and soil skeleton, as well as a finite thickness of a permeable seabed layer.

1. INTRODUCTION

Among all the environmental loads usually considered in the design procedure for offshore submarine pipelines buried in seabed sediments, the wave-induced pore-pressure – besides the hydrostatic one – plays one of the most important factors. A non-vertical distribution of the wave-induced pore-pressure with depth is responsible for creating the wave-induced pore-pressure gradient which, in turn, can cause instability of an upper part of the seabed layer, soil liquefaction, and consequently – a pipeline floatation which normally leads to a serious failure of a submarine pipeline. Even if there is no soil liquefaction in the close proximity of the pipeline this is also the case very relevant for engineering practice. The oscillating wave-induced pore-pressure distribution with depth induces an oscillating wave-induced pore-pressure gradient around the pipeline which results in an oscillating resultant force acting on the pipeline.

A vertical component of the resultant force, acting upwards and trying to lift up the pipeline from the seabed, is called the wave-induced uplift force or the hydrodynamic uplift force, contrary to the hydrostatic uplift force which is described simply by the Archimedes' law. The hydrodynamic uplift force has a character of an oscillating force due to also oscillating character of surface wave loading, and is comparable to the displaced water weight (Monkmeyer *et al.*, 1983; Cheng and Liu, 1986; Magda, 1997) if the pipeline is located relatively close to the seabed surface. An inadequate design, or even omitting the

* Marine Civil Engineering Department, Faculty of Environmental Engineering, Technical University of Gdansk, Gdansk, Poland
** Department of Environmental and Civil Engineering, Faculty of Environmental Science and Technology, Okayama University, Okayama, Japan

influence of the hydrodynamic uplift force, can cause floatation of the pipeline, very often leading subsequently to costly failures and environmental catastrophes. Of course, the whole problem can be avoided by installing an over-sized pipe or a pipeline on such a depth in the seabed where the influence of the wave-induced pore-pressure is of a minor meaning but, this would certainly increase the total costs of pipeline installation to an enormous amount and cannot be accepted for economic reasons. Therefore, it is essential to improve and to update continuously the knowledge on the interaction between water waves, seabed, and submarine pipeline buried in seabed sediments.

When a submarine pipeline is buried in a porous seabed and loaded by a continuous passage of surface waves, the solution to the wave-induced pore-pressure field around the pipeline, taking into account also the pore-pressure perturbation effects due to the presence of the pipeline impermeable body in the pore-pressure field, is not an easy task. In order to simplify this difficulty some researchers assumed that the seabed two-phase system (*i.e.*, porous soil skeleton and pore-water) could be treated as an incompressible medium. Under this assumption Lai *et al.* (1974), Liu and O'Donnell (1979), and Lennon (1983, 1985) investigated this problem using a numerical analysis. Liu and O'Donnell (1979) considered two different types of waves acting on the seabed, namely: monochromatic and solitary, and introduced the boundary integral equation method (BIEM) to solve the resulting integral equations. In a numerical solution procedure developed by Lennon (1983, 1985) the pore-pressure distribution on the pipeline was calculated using also the boundary integral equation method. By using the conformal mapping method, MacPherson (1978) and McDougal *et al.* (1988) presented an analytical solution for the case of an infinite thickness of the seabed layer (*i.e.*, half-space), whereas Monkmeyer *et al.* (1983), by using the 'image pipes' approach, found a similar solution which can be also applicable for a finite thickness of the seabed layer.

The common feature of all the studies mentioned above is that the effect of compressibility of both the pore-fluid and the soil skeleton was neglected by assuming the total incompressibility of the two-phase system. In such a case, the governing problem is described only by a very simple partial differential equation called the Laplace's equation. However, this equation is able to describe only the geometry of the problem, thereby making the problem independent on soil and pore-fluid parameters.

The first works considering a compressible seabed two-phase medium and a submarine pipeline totally buried in it, was published by Bobby *et al.* (1979) and Cheng & Liu (1986) who used the finite element method and the boundary integral equation method, respectively, in their analyses. Their works, however, have some important disadvantages that limit their practical applications. Magda (1992[a], 1992[b]) presented an analytical way of solution to the question of the hydrodynamic uplift force and, recently, Magda (1995, 1996, 1997) extended the work by Cheng and Liu (1986), by performing a wide numerical (FEM) parameter study and introducing a simple formula as a practical engineering tool for defining a possibly maximum value of the hydrodynamic uplift force. It was shown by Magda (1997) that the maximum wave-induced uplift force can be as much as even few times larger than the magnitude of the buoyant force due to the weight of water displaced (*i.e.*, hydrostatic uplift force) when real soil and pore-fluid parameters (among others: compressibility and permeability) are considered for the analysis. Simultaneously, the predominant meaning of the solution obtained for the compressible model was clearly indicated in comparison with the potential solution.

Taking into account the observed differences between theoretical and experimental results reported by Phillips *et al.* (1979), Monkmeyer *et al.*, 1983, and McDougal *et al.* (1988), it can be concluded that in order to obtain a possibly natural and accurate picture of the dynamic behaviour of a submarine pipeline buried in sandy seabed sediments it is necessary to perform an analysis based on:

- a theory of the wave-induced pore-pressure, in which some important and decisive soil skeleton and pore-fluid physical parameters (*e.g.*, compressibility) are taken into account,
- a theory, for which the solution derived for a finite-thickness permeable layer exists, or – if such a solution is rather difficult to derive analytically – a numerical method (*e.g.*, finite element method) where the imposition of realistic geometrical boundary conditions belongs to a normal computational procedure,
- input data adequate to these 'in-situ' which accompany natural sites or experimental sandy seabed models.

Comparing with large-scale modelling, small-scale tests are relatively less expensive, normally it is easier to perform them under the well-controlled way (*e.g.*, creating a homogeneous sand model) but, on the other hand, they can have some disadvantages because they are not very much recommended for the application of a real-shaped wave conditions because models are too small to avoid the combined influence of the side-wall boundary conditions and the asymmetry in wave loading conditions. Nevertheless, this problem can be overcome by introducing a water-table vertical oscillating movement instead of the wave-shaped water surface motion above the seabed model. It has to be noticed that the water loading by means of the water-table oscillating movement in the pipeline cross-section plane can be also related to the wave-shaped water surface motion with the respect to the longitudinal pipeline axis. Thereby, this type of water loading seems to be also very relevant to the engineering practice; this was also the reason and motivation to investigate this special case of water loading experimentally and numerically in the present study.

2. DEFINITION OF THE PROBLEM

2.1. Wave-induced pore-pressure and hydrodynamic uplift force

Considering a porous seabed (*e.g.*, sandy sediments), the wave-induced bottom pressure oscillations have a direct and continuous influences on changes of the pore-pressure within the seabed medium. Respectively to the *initial hydrostatic pore-pressure* distribution, which is a simply continuation of the hydrostatic pressure distribution in the water above the seabed, defined by a still water level, one can distinguish:

- Case (a), where an *over-pressure* or *positive pressure* is induced in the seabed due to the passage of the wave crest above the considered vertical profile,
- Case (b), where an *under-pressure* or *negative pressure* is induced in the seabed due to the passage of the wave trough above the considered vertical profile (Fig. 1).

In both cases these additional elements of the pore-pressure due to wave action are very often described using one common term, *i.e.* the *wave-induced pore-pressure.* The wave-induced pore-pressure distribution with depth in the seabed is not a vertical one due

to some pore-pressure attenuation and phase-lag effects. It means that a certain wave-induced pore-pressure vertical gradient exists in the upper layer of the seabed. Should one assume now the existence of a submarine pipeline buried in a porous and permeable seabed, the pipeline will be exposed to a non-uniform distribution of the wave-induced pore-pressure on its outer surface. This will result in the wave-induced force acting to the pipeline, the magnitude and the direction of which alter within one cycle of wave loading and they are repeated periodically from one wave cycle to another one.

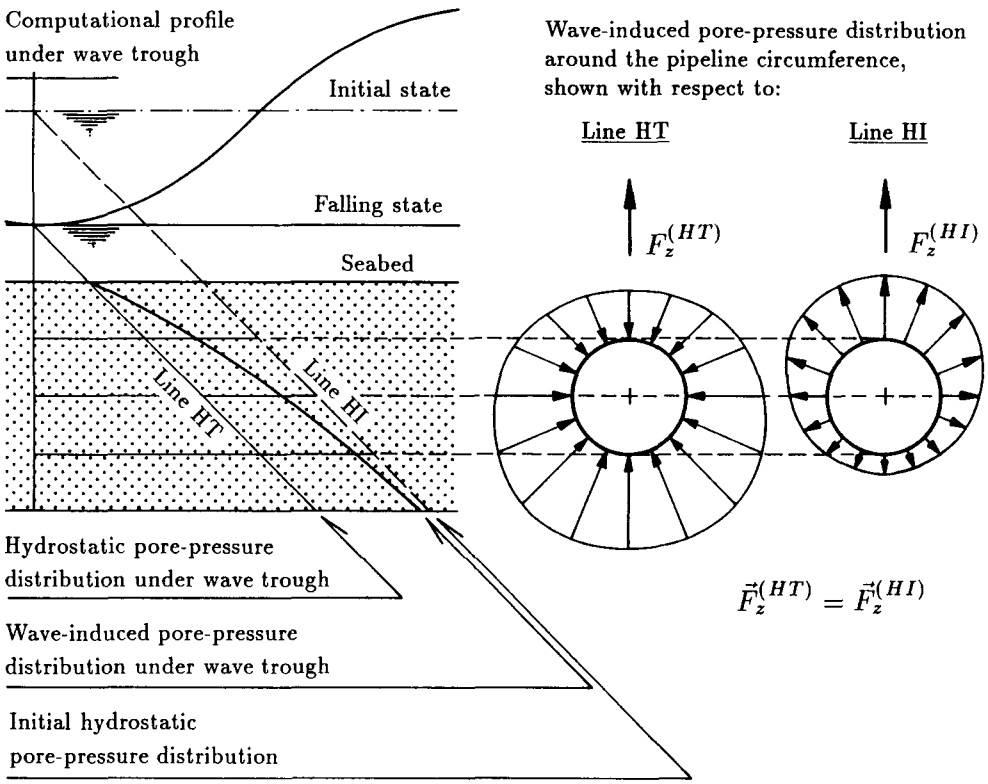

Fig. 1 Sketch definition of the wave-induced pore-pressure distribution with depth and around the pipeline buried in seabed sediments

Besides the always existing hydrostatic uplift force (buoyancy), the vertical and upwards directed component of the resultant hydrodynamic force is called the *hydrodynamic uplift force* or *wave-induced uplift force*. A positive value is normally assigned to this force when the passage of the wave trough tends to lift up the pipeline out of the seabed. The hydrodynamic uplift force plays a very important role and has to be taken into account during the design of a submarine pipeline buried in seabed sediments. If the hydrodynamic uplift force is large enough the pipeline vertical stability factor can be decreased up to a certain critical level, a serious vertical displacement of the pipeline can appear, leading very often to the exposure of the pipeline onto the seabed bottom, and later on – this can lead even to the pipeline floatation up to the sea level and sometimes the pipeline breakout can take place.

2.2. Mathematical definition of the governing problem

Soil domain

Under plain-strain conditions, the following two equations, describing elastic deformations of the soil skeleton, together with the 'storage' equation constitute the coupled problem and they can be written as:

$$G_s\left(\frac{\partial^2 u_x}{\partial x^2}+\frac{\partial^2 u_x}{\partial z^2}\right)+\frac{G_s}{1-2\nu_s}\frac{\partial}{\partial x}\left(\frac{\partial u_x}{\partial x}+\frac{\partial u_z}{\partial z}\right)=\frac{\partial p}{\partial x} \tag{1a}$$

$$G_s\left(\frac{\partial^2 u_z}{\partial x^2}+\frac{\partial^2 u_z}{\partial z^2}\right)+\frac{G_s}{1-2\nu_s}\frac{\partial}{\partial z}\left(\frac{\partial u_x}{\partial x}+\frac{\partial u_z}{\partial z}\right)=\frac{\partial p}{\partial z} \tag{1b}$$

$$\beta' n\frac{\partial p}{\partial t}+\frac{\partial}{\partial t}\left(\frac{\partial u_x}{\partial x}+\frac{\partial u_z}{\partial z}\right)=\frac{k}{\gamma}\left(\frac{\partial^2 p}{\partial x^2}+\frac{\partial^2 p}{\partial z^2}\right) \tag{1c}$$

where: p is the wave-induced pore-pressure, u_x and u_z are the horizontal and vertical displacements of soil skeleton, respectively, G_s is the shear modulus of soil, ν_s is the Poisson's ratio of soil, k is the coefficient of isotropic permeability of soil, γ is the unit weight of pore-fluid, β' is the compressibility of pore-fluid, n is the porosity of soil, x and z are horizontal and vertical coordinates of the Cartesian coordinate system, respectively, and t is the time.

The above presented set of coupled partial differential equations was already used by many researchers (*e.g.*, Madsen, 1978; Yamamoto *et al.*, 1978; Okusa, 1985; Magda, 1992[a], 1992[b], 1994, 1995, 1996, 1997; Nago and Maeno, 1984, 1986[a], 1986[b]; Maeno and Nago, 1988, 1991, 1996) in their analytical and numerical analyses of the seabed-wave and seabed-wave-structure interactions. A linear stress-strain relationship for the soil is represented by Eq. (1a) and Eq. (1b) which are formed from the equilibrium condition in the x- and z- direction, respectively. Eq. (1c) reflects the continuity principle incorporating the Darcy's law of fluid flow through a porous medium. The inertia forces are small for this type of problem (Cheng and Liu, 1986) and therefore the body forces are set to zero and neglected in the present analysis. Using proper set of input data, Eqs. (1a) to (1c) can bed used to simulate any of the following three models of the two-phase system compound of soil skeleton and pore-fluid phases, *i.e.*:

- totally incompressible two-phase system (INCOMP model),
- partially incompressible/compressible two-phase system, where the soil skeleton is assumed incompressible and the pore-fluid compressible (COMP-P model) or vice versa (COMP-S model),
- totally compressible two-phase system (COMP-PS model).

Seabed saturation conditions, especially in case of the vertical stability analysis of a submarine pipeline buried in sandy seabed sediments, form a very important factor – they are responsible to a great extent for the wave-induced pore-pressure gradient in the upper part of the seabed where the pipeline is normally installed. Under realistic conditions, the pore-fluid is represented by a two-phase medium where the water and air components can be distinguished. However, in order to simplify and enable the calculation procedure, the compressibility of this two-phase medium is defined by a very convenient, from the engineering point of view, formula proposed by Verruijt (1969) and applied by many other researchers (*e.g.*, Madsen, 1978; Yamamoto *et al.*, 1978; Okusa, 1985; Magda, 1992[a],

1992(b), 1994, 1995, 1996, 1997). This formula, describing the pore-fluid compressibility with respect to saturation conditions, represented by the degree of saturation, has the following form:

$$\beta' = \beta + \frac{1 - S}{P_{ab}} \qquad \text{for} \qquad S \geq 0.85 \tag{2a}$$

in which:

$$P_{ab} = P_{at} + \gamma h \tag{2b}$$

where: β' is the compressibility of pore-fluid, β is the compressibility of pure water, S is the degree of saturation, P_{ab} is the absolute hydrostatic pressure, P_{at} is the atmospheric pressure, γ is the unit weight of sea water, and h is the water depth.

Table 1 shows the results of illustrative computations of the pore-fluid compressibility, where the following values were assigned for the input data: water depth $h = 10\,\text{m}$ (*i.e.*, absolute pressure $P_{ab} \equiv P = 101.325 + 1.025 \cdot 9.81 = 201.9\,\text{kPa}$), compressibility of pure water $\beta = 4.2 \times 10^{-7}\,\text{m}^2/\text{kN}$, and soil porosity (total) $n \equiv \lambda = 0.4$).

Table 1
Dependence of the pore-fluid compressibility on the degree of saturation [after Eq. (2a) with (2b)]

Degree of saturation S [-]	Compressibility of pore-fluid β' [m^2/kN]
1.000	4.20×10^{-7}
0.999	5.37×10^{-6}
0.99	4.99×10^{-5}
0.98	9.95×10^{-5}
0.95	2.48×10^{-4}

Pipeline domain

The system of coupled equations describing the governing problem within the pipeline-wall material is even simpler than in case of the soil domain. Being still in the range of linear-elastic deformations and assuming that the pipeline solid wall (*e.g.*, made of steel or concrete) creates an impermeable boundary condition, only two equilibrium equations are required. They can be easily obtained from the first two equations [*i.e.*, Eq. (1a) and Eq. (1b) describing the governing process in the soil domain], after neglecting the pore-fluid terms and replacing the values of G_s and ν_s, assumed for the soil skeleton, by proper values of G_p and ν_p, respectively, characteristic for the pipeline-wall material. The third continuity equation [Eq. (1c)] has not any practical meaning as far as the impermeable and solid pipeline-wall domain is concerned and therefore disappears from the equation system assigned for the pipeline domain.

2.3. Numerical formulation of the problem

Equations for the finite element method

The system of coupled equations Eqs. (1a) to (1c) was discretized using the Galerkin finite element method. Due to the geometry of the problem, the four-node isoparametric elements were chosen. The time-approximation was obtained using the 'backward scheme' which is, in a variety of engineering problems, estimated to be 'well-behaved' by showing no oscillations in numerical results. Because of their lengthy form the system of discretized equations will not be cited here; they can be found in some works, *e.g.*, published by Nago and Maeno (1984) or Magda (1996).

Time- and space-discretization

Magda (1996) performed several test computations in order to demonstrate the model utility and check numerical accuracy influenced by the time- and space-discretization as well as the quadrature rule for numerical integration. It was shown that reasonably good results can be obtained when the whole period of oscillations is divided into 20 time-steps, which implies from 3 to 10 (depending highly on the relative compressibility of the two-phase system) oscillation periods necessary to achieve numerical stability of the results.

A local refinement of the FE-mesh of the soil domain in the vicinity of the buried submarine pipeline is particularly important when the wave-induced pore-pressure values computed in all nodes from the pipeline outer circumference are used to compute the wave-induced uplift force. A sufficiently acceptable local refinement of the FE-mesh is shown in Fig. 2.

Magda (1996) gave also some recommendations concerning dimensions of the numerical 'sand box' suited for the numerical analysis with a wave-shaped type of water loading. However, assuming the oscillating vertical water movement, dimensions of the numerical 'sand box' can be set arbitrary, for example, according to the shape of the real 'sand box' foreseen for small-scale laboratory experiments.

Geometry, boundary conditions and loading

Geometry of the numerical 'sand box' is represented by the width of the box B_{box} and the height of the box H_{box}. The outer diameter of the submarine pipeline is denoted by D, whereas the depth of burial (counted from the seabed surface to the top of the pipeline) is denoted by b (Fig. 3).

The geometrical boundary conditions (essential and natural), used in the governing problem, are also schematically illustrated in Fig. 3. The rigid vertical walls and the horizontal bottom of the numerical 'sand box' were simulated by a constrained movement of the soil skeleton (*i.e.*, $u_x = 0$ and/or $u_z = 0$). The impermeability condition was achieved by setting to zero the wave-induced pore-pressure gradient, perpendicular to the vertical walls or horizontal bottom (*i.e.*, $\partial p/\partial x = 0$ or $\partial p/\partial z = 0$).

Assuming that the buried submarine pipeline is made of rigid and impermeable material, the wave-induced pore-pressure gradient (perpendicular to the pipeline-wall surface) has to fulfill the the following condition:

$$\frac{\partial \bar{p}}{\partial r} = 0 \qquad \text{on the pipeline outer surface } (i.e.,\ r = r_p) \tag{3}$$

where: r is the linear coordinate (normal to the pipeline surface) in the polar coordinate system with its origin in the centre of the pipeline cross-section.

Number of nodes : 275
Number of elements : 236

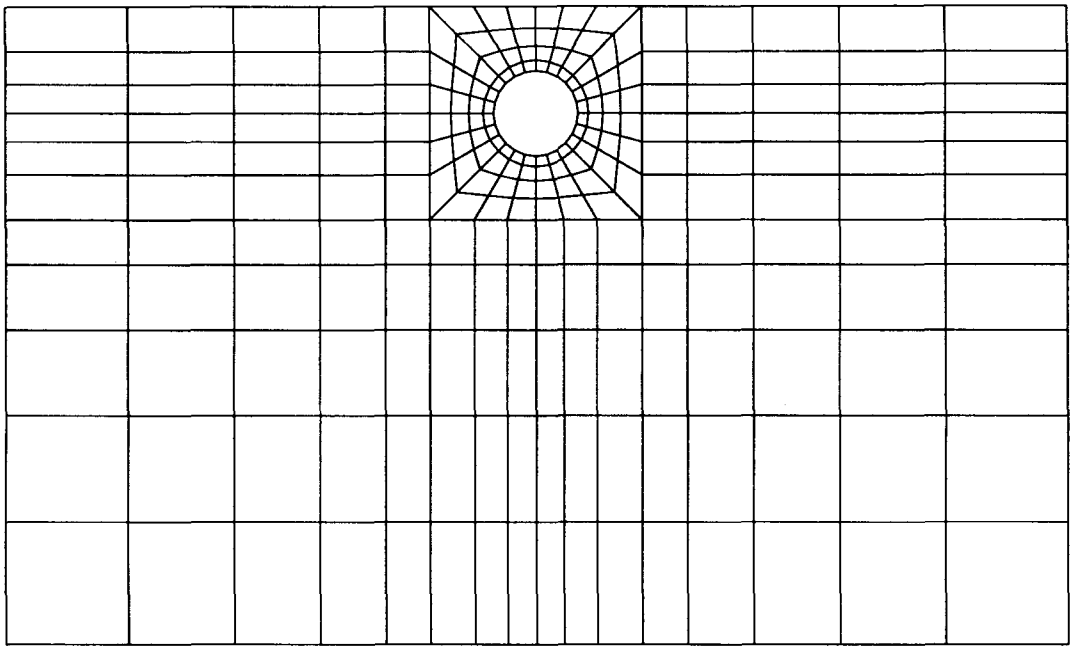

Fig. 2 Finite-element mesh pattern in the vicinity of the buried submarine pipeline

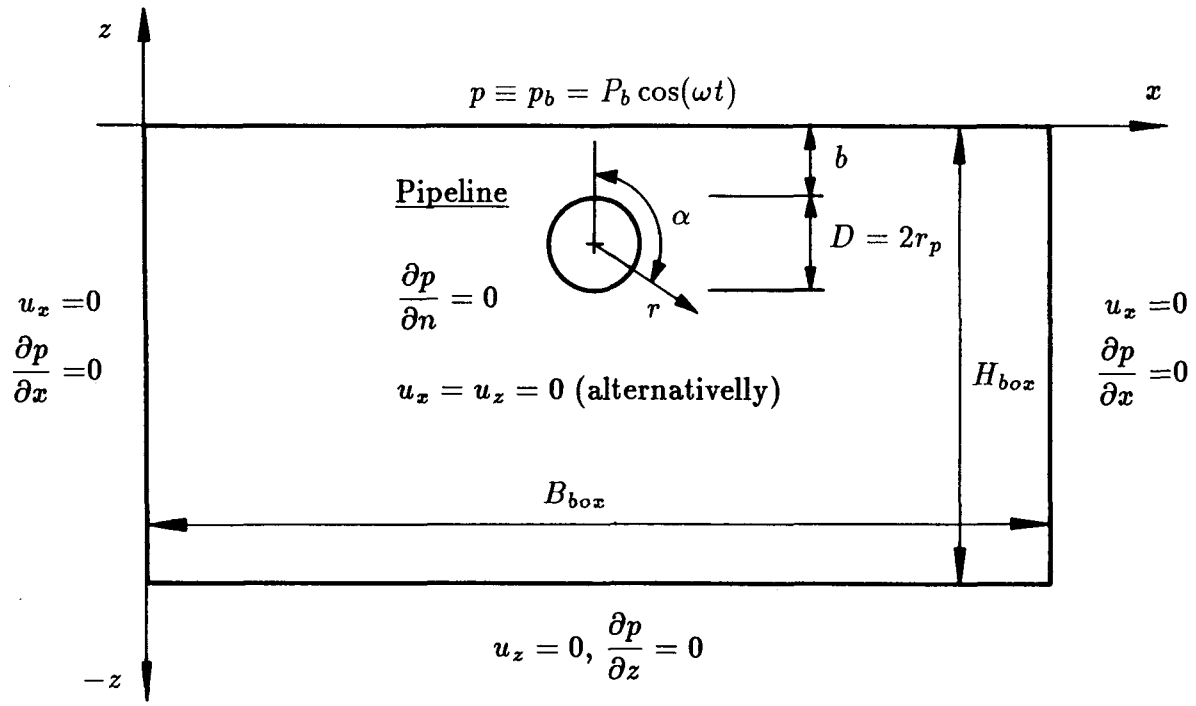

Fig. 3 Illustration of boundary conditions imposed on soil skeleton and pipeline displacements as well as water loading and wave-induced pore-pressure gradient

The fixed position of the pipeline in the 'sand box' was modelled by assuming the constrained conditions $u_x = u_z = 0$ in all nodes from the pipeline domain.

As far as the water-loading boundary condition is concerned, the wave-induced bottom pressure acting cyclically at the seabed bottom was assumed to result from the oscillating water-table vertical movement:

$$p_b = P_b \cos(\omega t) \tag{4a}$$

in which:

$$P_b \simeq \gamma A \tag{4b}$$

where: p_b is the oscillating bottom pressure, P_b is the amplitude of oscillating bottom pressure, γ is the unit weight of water, A is the amplitude of water-table oscillations, ω is the angular velocity of pressure oscillations, and t is the time.

Input data

The following main input data were used in the numerical analysis: width of the numerical 'sand box' $B_{box} = 1.0\,\text{m}$, height of the numerical 'sand box' $H_{box} = 0.6\,\text{m}$, pipeline outer diameter $D = 0.1\,\text{m}$, depth of burial of the pipeline in the numerical 'sand box' $b = 0.05\,\text{m}$ (counted from the upper surface of the box to the top of the pipeline), still water level (static water depth) $h = 1.1\,\text{m}$, amplitude of the vertical water-table oscillations $A = 0.4\,\text{m}$, period of oscillations of the vertical water-table movement $T = 0.5;\ 1.0;\ 2.0\,\text{s}$, shear modulus of soil $G_s = 3.5 \times 10^4\,\text{kN/m}^2$, Poisson's ratio of soil $\nu_s = 0.45$, soil porosity $n = 0.4$, coefficient of isotropic permeability of soil $k = 1.5 \times 10^{-3}\,\text{m/s}$, compressibility of pure water $\beta = 4.2 \times 10^{-7}\,\text{m}^2/\text{kN}$, degree of saturation $S = 0.90 - 1.0$.

2.4. Results of numerical computations

As it was mentioned before, a non-vertical distribution of the wave-induced pore-pressure with depth produces a certain gradient of the wave-induced pore-pressure in the upper part of the seabed sediments. Therefore, the wave-induced pore-pressure distribution along the pipeline circumference is not uniform. This can be clearly seen from Fig. 4 where qualitative distributions of the wave-induced pore-pressure around the pipeline are shown with respect to four different saturation conditions, *i.e.*: $S = 1.0$, 0.99, 0.98 and 0.96. Only the first distribution, obtained for $S = 1.0$ is almost uniform; all others show a higher under-pressure (with respect to the initial hydrostatic pressure distribution with depth) in the upper part than in the lower part of the pipeline cross-section. However, in all four cases the distributions are symmetrical respectively to the vertical axis that goes through the pipeline centre. This is due to water loading in the form of water-table vertical oscillations which is, of course, dependent on time (a sinusoidal variation with time is assumed), but independent of x-position; it means that the water loading induces always a uniform bottom pressure; in other words – the bottom pressure induced at a certain time is the same in all points of the bottom surface.

For the presentation and comparison purposes it is convenient to introduce the wave-induced pore-pressure in a dimensionless form, given with respect to the amplitude of the bottom pressure:

$$\bar{p} = \frac{p}{P_b} \tag{5}$$

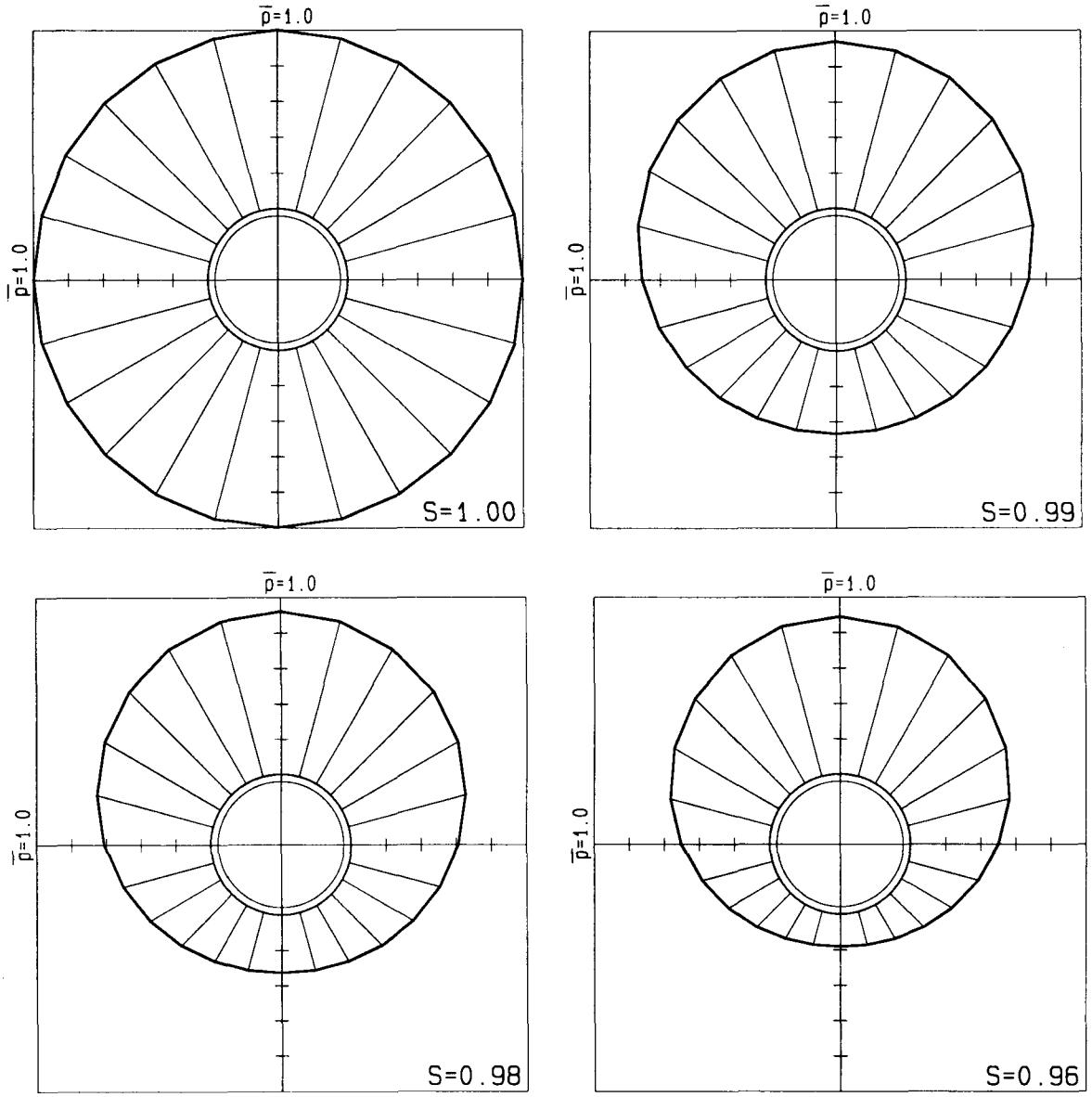

Fig. 4 Wave-induced pore-pressure distribution around the pipeline circumference, computed for different soil saturation, and $t = T/2$ (water-table loading: $T = 1\,\mathrm{s}$, $h = 1.1\,\mathrm{m}$; sand: $G_s = 3.5 \times 10^4\,\mathrm{kN/m^2}$, $k = 0.00015\,\mathrm{m/s}$; COMP-PS model)

where: $\bar{p}$ is the wave-induced pore-pressure (dimensionless), p is the wave-induced pore-pressure (dimensional), and P_b is the amplitude of the bottom pressure. This form makes the relative wave-induced pore-pressure independent of the wave height.

A detailed picture of the wave-induced pore-pressure values in some very characteristic points of the pipeline circumference, influenced by different soil saturation conditions, is presented in Fig. 5. Point No. 2 denotes the position on the top of the pipeline, point No. 6 denotes the position at the bottom of the pipeline cross-section; points No. 3, 4, and 5 are placed between point No. 2 and point No. 6, equally separated from each other on the pipeline circumference. The wave-induced pore-pressure at the top of the pipeline (point No. 2, $z = -0.05\,\mathrm{m}$) shows relatively the smallest attenuation for the whole range of the degree of saturation assumed for the analysis. The deeper-situated characteristic point

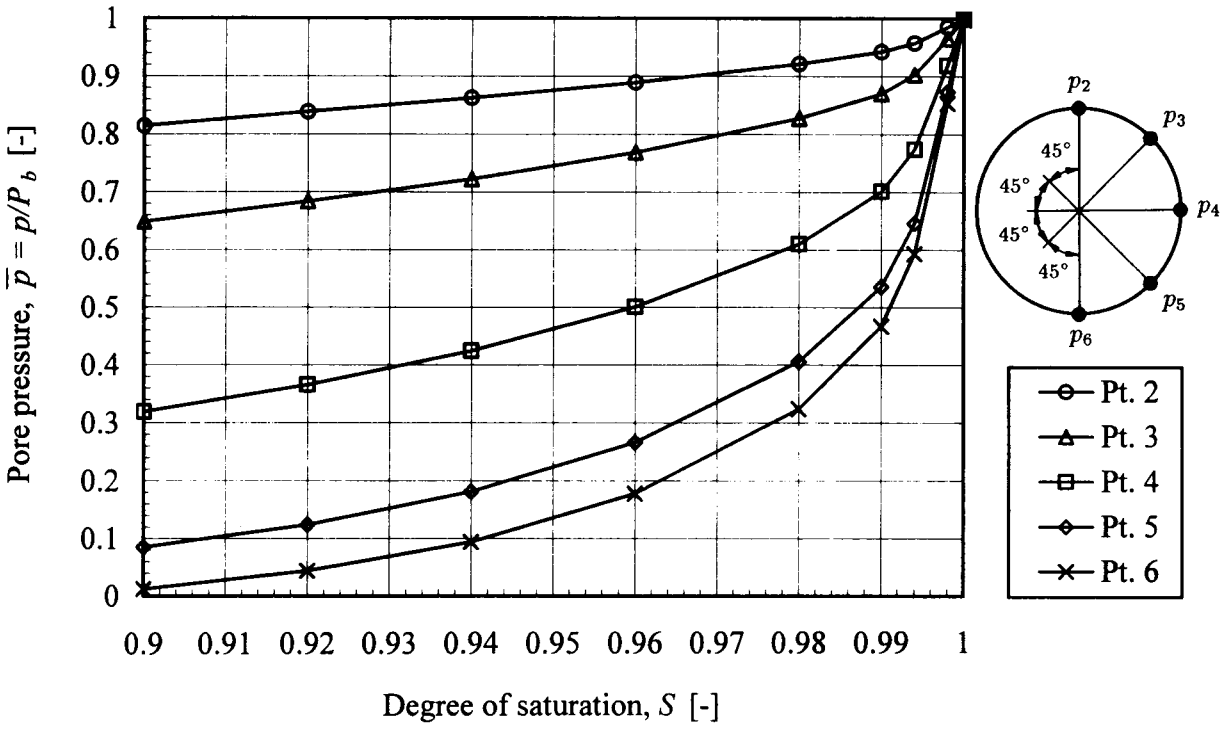

Fig. 5 Wave-induced pore-pressure in 5 characteristic points of the pipeline cross-section, computed for different soil saturation, and $t = T/2$ (water-table loading: $T = 1\,\mathrm{s}$, $h = 1.1\,\mathrm{m}$; sand: $G_s = 3.5 \times 10^4\,\mathrm{kN/m^2}$, $k = 0.00015\,\mathrm{m/s}$; COMP-PS model)

on the pipeline circumference is the higher attenuation of the wave-induced pore-pressure can be observed. Assuming a constant value for the combined pore-fluid and soil skeleton compressibility in the whole soil domain, differences in the pore-pressure attenuation in the characteristic points of the pipeline circumference result from: (1) different depths in the 'sand box', and (2) the elongation of the pore-fluid seepage way due to the pipeline impermeable body that acts like a barrier for the wave-induced pore-pressure propagation in sandy sediments.

3. SMALL-SCALE LABORATORY EXPERIMENTS

As it was stated before, a series of small-scale laboratory experiments was planned to investigate a complex system of the dynamic behaviour of the submarine pipeline buried in sandy seabed sediments. The present report deals only with the case of fixed pipeline (*i.e.*, firmly connected with the test container) and water-table harmonic oscillations above the seabed model.

3.1. Test facilities and layout

For the experiment, a vertical two-dimensional model (rectangular container) shown in Fig. 6 was used. The container has the following dimensions: $B_c = 1.0\,\mathrm{m}$ (length), $H_c = 0.7\,\mathrm{m}$ (height), and $W_c = 0.4\,\mathrm{m}$ (width). The container was filled with highly

saturated standard sand. The thickness of the sand layer was $H_s = 0.6\,\mathrm{m}$. On the top of the container, an oscillating water column was installed. The still water depth, measured from the sand surface, is equal to 1.1 m. The water surface oscillations in the column were generated by an oscillating air-pressure acting on the water surface. The air-pressure oscillations, in turn, were generated by a mechanical generator. The amplitude of the cyclic water-pressure oscillations was about $A = 0.4\,\mathrm{m}$. Three different periods of oscillations were investigated, namely: $T = 0.5$, 1 and 2 s.

A cylindrical and hardly deformable element of the pipeline, made of perspex (lucid acrylic rasin), was buried and fixed firmly between the front and the back wall of the container. The outer diameter of the pipeline testing section equals $D = 0.10\,\mathrm{m}$. The depth of burial of the pipeline equals $b = D/2 = 0.05\,\mathrm{m}$.

Pore-pressure oscillations were measured at 5 points (Pts. 2 to 6) equally spread along the pipeline half-circumference in the middle of the pipeline section, and additionally for comparison purposes – in the back wall of the container (Pt. 1) for monitoring the water-pressure just above the sand surface. The measuring cross-section of the pipeline is shown in Fig. 7. Only one half of the pipeline circumference was instrumented because of the symmetry of the whole system.

Water-pressure oscillations in the water above the sand surface, and the pore-pressure oscillations around the pipeline circumference were transmitted to the pressure transducers by 6 plastic connecting tubes with a practically non-deformable cross-section (in order to avoid measuring errors that could be caused by changing the inside volume of the tube respectively of the inner water-pressure).

Each of 5 openings in the pipeline wall in the measuring cross-section was covered by a protective sheet of a very fine metal mesh to protect the opening against clogging and also to avoid the inflow of fine-sand particles into the measuring volume of the system.

The data acquisation system consists of three main units: amplifier, analog-to-digital converter and data recording sytem (floppy-disc recorder and multi-pen recorder), connected in series (see Fig. 6).

3.2. Sand parameters

The container was filled with fine-grained sand ("Toyoura" standard sand: $d_{50} = 0.25\,\mathrm{mm}$). The specific weight of the sand is equal to 2.65, the coefficient of isotropic permeability $k = 0.00015\,\mathrm{m/s}$, the porosity $n = 0.4$, the Poisson's ratio $\nu_s = 0.45$, and the shear modulus $G_s = 3.5 \times 10^4\,\mathrm{kN/m^2}$. All these values of soil parameters are characteristic for this type of sand which have been used already in many other similar small-scale experiments conducted at Okayama University (*e.g.*, Maeno *et al.*, 1996).

3.3. Test preparation procedure

The container was filled with water stepwise. Between the two following water filling, a certain volume of dried sand was dropped freely into the water to assure repeatedly uniform soil conditions for each new-established test. A careful preparation of the sand model required that the sand surface had been always kept below the water surface. This was necessary to achieve a possibly high degree and uniformity of soil saturation.

Its very difficult to measure soil saturation conditions very precisely. It was clear that the sand bed was partly saturated. However, one of the most important goals in the test preparation procedure was to create the sand saturation as high as possible. Therefore, an

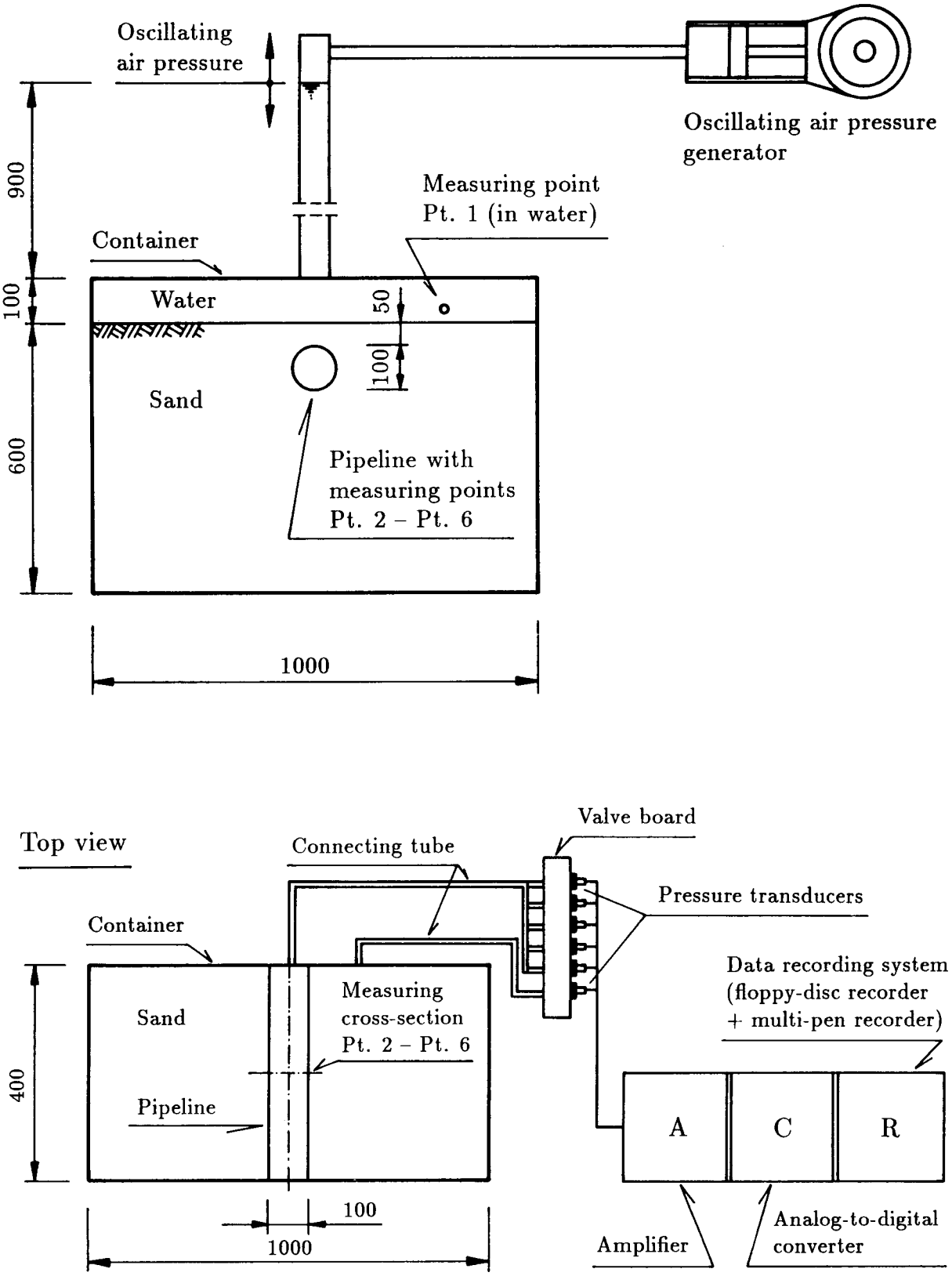

Fig. 6 Experimental facilities for small-scale modelling of the soil-water-pipeline interaction

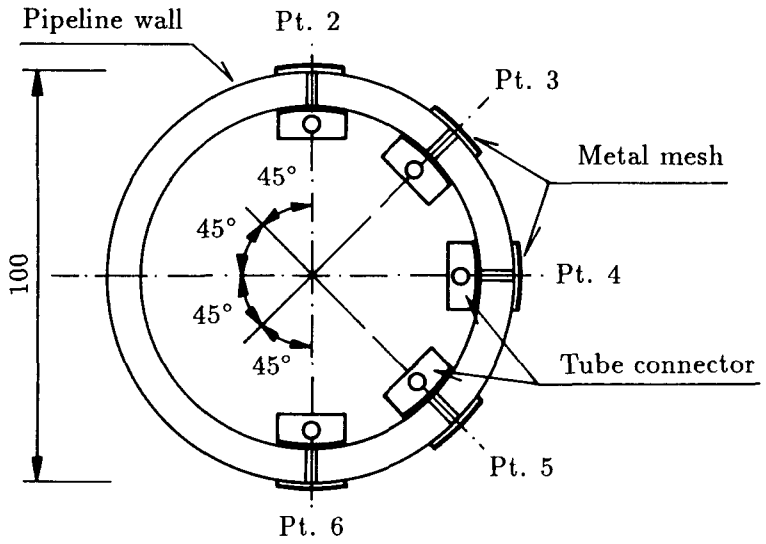

Fig. 7 Detailed sketch of the measuring cross-section of the pipeline

additional unit with a vibrating needle was used to release entrapped air-bubbles from the soil model. This procedure helped also in preparing a uniformly densified sand model.

3.4. Experimental procedure

Pressure measurements were conducted in the form of short series at the beginning of each test and after 1,000 min of continuous loading of the cyclically generated water-pressure oscillations. It was possible to record pressure data gained from each of 6 channels in 1280 measuring time-points. The sampling frequency $f = 100$ Hz implied a continuous data recording from 6.4 ($T = 2$ s) to 25.6 ($T = 0.5$ s) sequential pressure oscillations. After 1,000 min of a continuous run, the experiment was stopped.

All together three experiments were performed: SAND-1 ($T = 1$ s), SAND-2 ($T = 0.5$ s) and SAND-3 ($T = 0.5$, 1 and 2 s). A new seabed model was always prepared for each experiment. There was not any intentional differences in the preparation procedure of the seabed model.

3.5. Results of measurements and comparison with the numerical model

Fig. 8 illustrates a short part (length of approximately one period of oscillations) of the typical pressure recording from 6 channels. It is very characteristic to observe a certain pore-pressure attenuation for deeper-placed measuring points. The pore-pressure attenuation is also accompanied by the phase-lag phenomenon in pressure oscillations.

The main target of the experimental part of the presented analysis on the dynamic behavior of submarine pipeline buried in seabed sediments was to indicate the importance of the combined pore-fluid and soil skeleton compressibility in the estimation of the hydrodynamic uplift force acting on the buried submarine pipeline. This could be possible to achieve by showing the predominant influence of highly (but not fully) saturated seabed sediments on the magnitude of the hydrodynamic uplift force.

As it was mentioned before, it is extremely difficult, or almost impossible, to identify soil saturation conditions qualitatively with a high accuracy. Therefore, a comparison

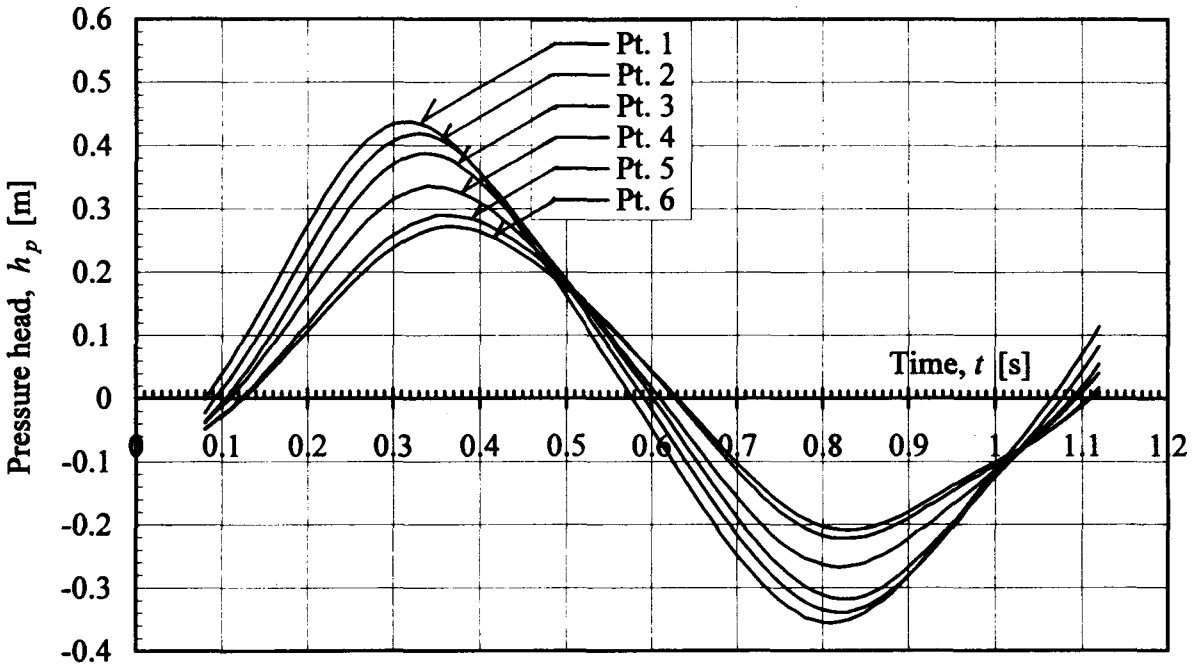

Fig. 8 Typical recording from the pore-pressure transducers in the small-scale laboratory experiment with the pipeline buried in the 'sand box'. Test No. SAND-1 (wave-table loading: $T = 1\,\mathrm{s}$, $h = 1.1\,\mathrm{m}$, $A = 0.4\,\mathrm{m}$; sand: $G_s = 3.5 \times 10^4\,\mathrm{kN/m^2}$, $k = 0.00015\,\mathrm{m/s}$)

technique was used to clarify this problem as much as possible. The comparison was done by matching the appropriate experimental results with the respective numerical results.

The numerical results, used for the comparison purposes, are shown in Fig. 5 which illustrates the influence of soil saturation conditions on the pore-pressure computed in 5 characteristic points at time $t = T/2$. Each set of recorder data was used to compute 5 values (mean from 5 sequential oscillations) of pore-pressure recorded at the lowest state of loading (similarity with the wave trough). By matching 5 numerically obtained curves with 5 experimental mean values of pore-pressure, a picture of the distribution of the optimum degree of saturation in 5 characteristic measuring points can be easily obtained.

The results of the above described comparison procedure are shown in Fig. 9 (test no. SAND-1), Fig. 10 (test no. SAND-2) and Fig. 11 (test no. SAND-3). Each figure containes two curves obtained from the analysis of the data recorded at the beginning ($t = 0\,\mathrm{min}$) and at the end ($t = 1{,}000\,\mathrm{min}$) of a singular experiment with continuous $1{,}000\,\mathrm{min}$ long water loading of the seabed model.

In an ideal case, when the whole sand model has uniform saturation conditions (*i.e.*, the degree of saturation is constant), the distribution of the optimum degree of saturation through the all 5 characteristic points of the pipeline circumference should be vertical. Of course, experimental results show always a certain deviation from the ideal picture of the investigated phenomenon. Figs. 9 to 11 can only certify this statement.

However, it can be seen in Fig. 9 that the distribution of the optimum degree of saturation from the beginning ($t = 0\,\mathrm{min}$) of the experiment SAND-1 can be practically treated as vertical which can only confirms a well-done sand model preparation. The

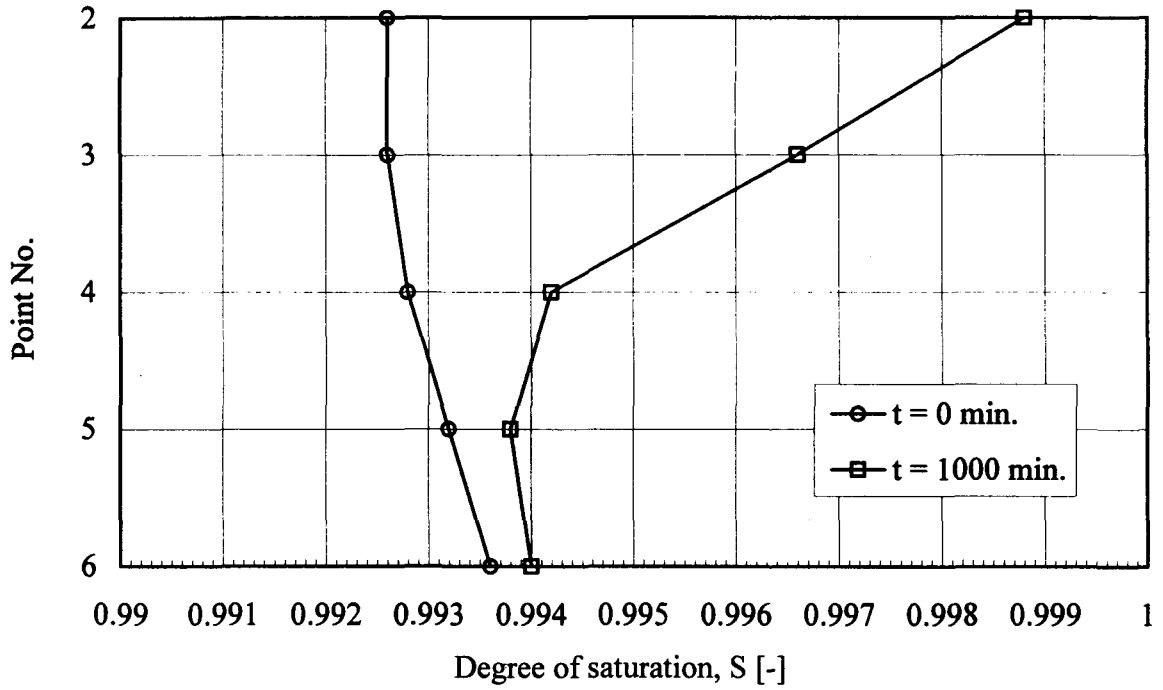

Fig. 9 Test No. SAND-1 (wave-TABLE loading: $T = 1\,\mathrm{s}$, $h = 1.1\,\mathrm{m}$, $A = 0.4\,\mathrm{m}$; sand: $G_s = 3.5 \times 10^4\,\mathrm{kN/m^2}$, $k = 0.00015\,\mathrm{m/s}$)

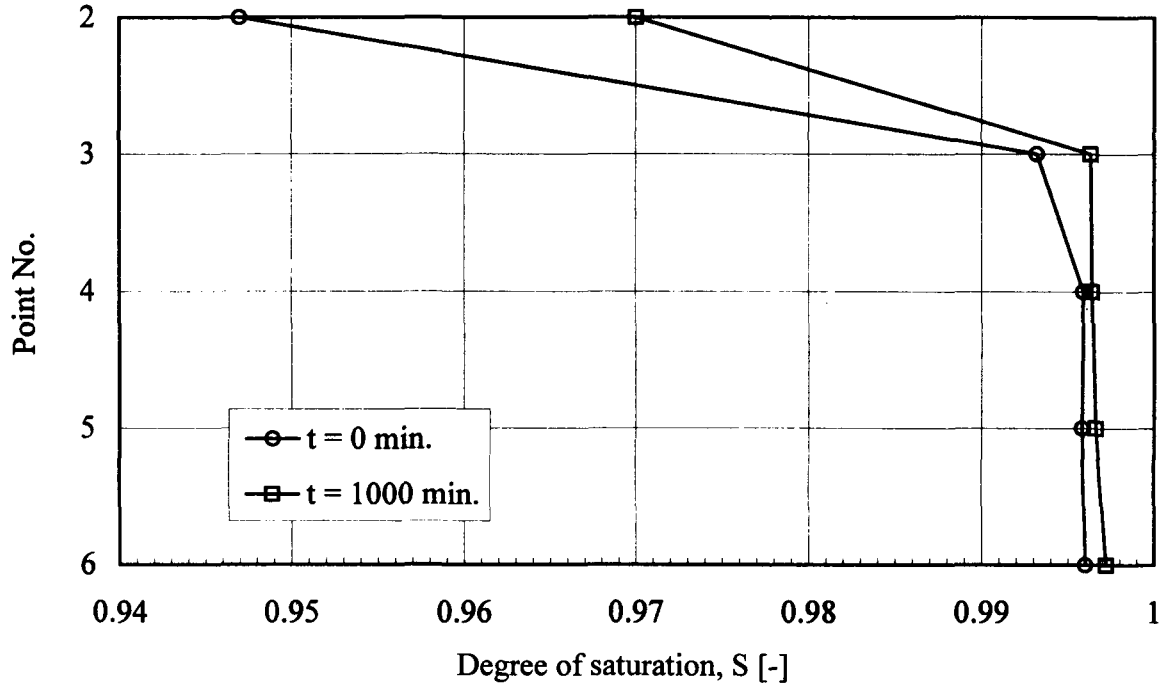

Fig. 10 Test No. SAND-2 (wave-TABLE loading: $T = 0.5\,\mathrm{s}$, $h = 1.1\,\mathrm{m}$, $A = 0.4\,\mathrm{m}$; sand: $G_s = 3.5 \times 10^4\,\mathrm{kN/m^2}$, $k = 0.00015\,\mathrm{m/s}$)

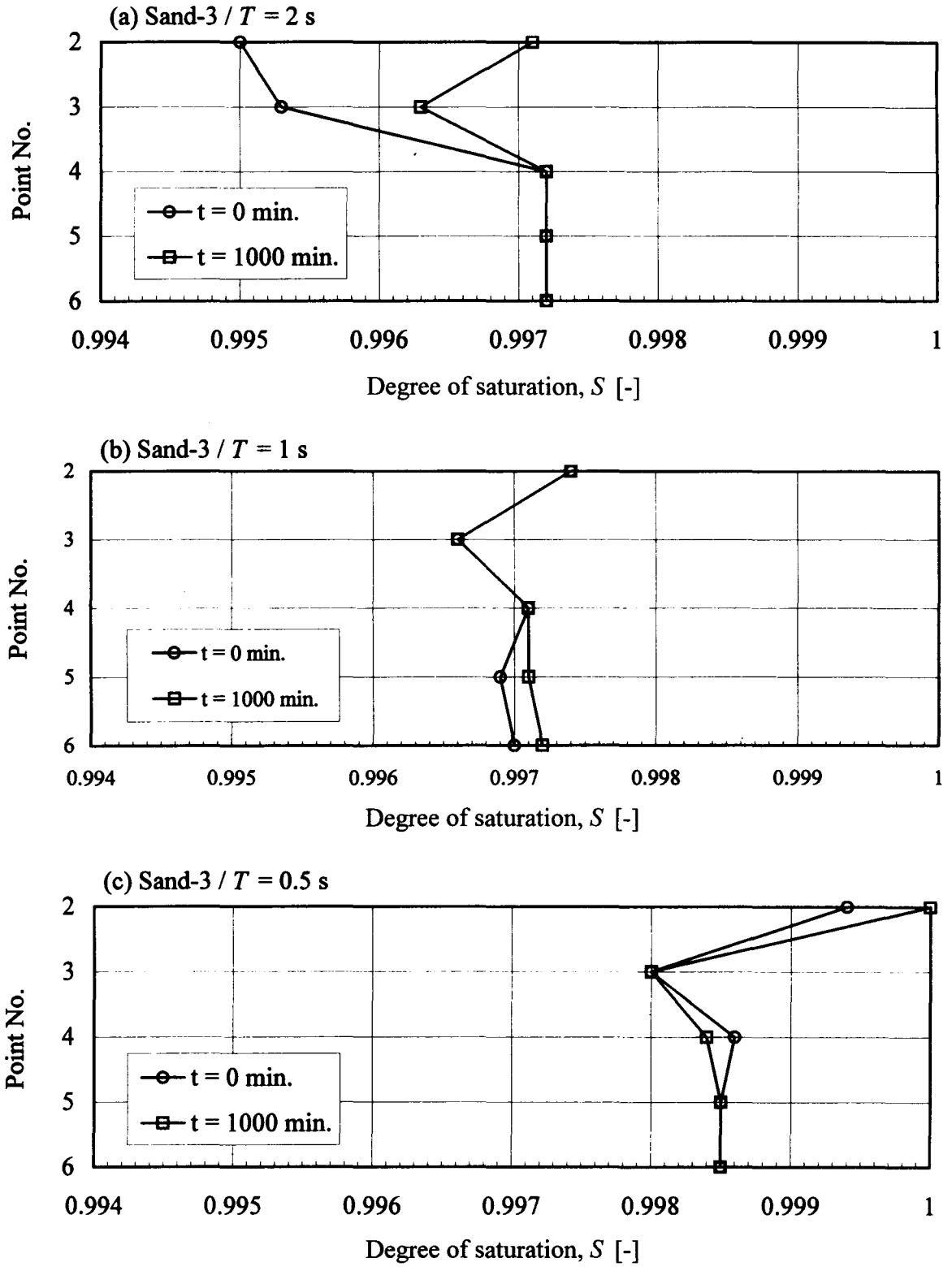

Fig. 11 Test No. SAND-3 (wave-TABLE loading: (a) $T = 2\,\mathrm{s}$, (b) $T = 1\,\mathrm{s}$, (c) $T = 0.5\,\mathrm{s}$, $h = 1.1\,\mathrm{m}$, $A = 0.4\,\mathrm{m}$; sand: $G_s = 3.5 \times 10^4\,\mathrm{kN/m^2}$, $k = 0.00015\,\mathrm{m/s}$)

difference between points Pt. 2 and Pt. 6 is very small and equal $\Delta S = 0.0011$. The second curve ($t = 1,000$ min) indicates the influence of a continuous water loading on the initial state of soil saturation. A relatively long time of cyclic loading increases the degree of saturation, at least in the upper soil layer; the difference between the two curves in point Pt. 2 is equal to $\Delta S = 0.0063$ whereas in point Pt. 6 only $\Delta S = 0.0004$. This is probably because it is easier to release still remaining air-bubles from the upper part of the seabed than from the lower situated deposits. Generally, a very high degree of saturation ($S > 0.992$) of the seabed model was indicated.

Even higher values of the degree of saturation ($S > 0.996$) were found from the second experiment (test no. SAND-2, Fig. 10) but only in the lower part of the seabed model. Taking the upper part into account, a dramatic drop in saturation conditions can be observed; point Pt. 2 indicates $S = 0.947$. Only man-made errors during the preparation of the new sand model seem to be a rational explanation of such strong differences. In spite of this fact, a general improvement of soil saturation conditions can be seen when comparing the results from the beginning and the end of test no. SAND-2.

The last experiment (test no. SAND-3) was more complex than the former because, using one set-up of the sand model, three different periods of oscillations were tested, starting from $T = 2$ s (Fig. 11a) through $T = 1$ s (Fig. 11b) to $T = 0.5$ s (Fig. 11c). Fig. 11a indicates very clearly the increase in the optimum degree of saturation in the upper half of the seabed sediments, after 1,000 min of continuous water loading; saturation conditions in the lower half does not change visibly. The results gained from the end of the test with $T = 2$ s should show high similarity with the results obtained from the beginning of the following test with $T = 1$ s. This is actually true and can be certified when comparing Figs. 11a and 11b. 1,000 min of water loading oscillations with $T = 1$ s did not cause any improvement of the saturation conditions in the upper half of the sand model. This time, however, only a small improvement ($\Delta S = 0.002$) in the lower half can be seen.

Comparing the results from the end of the test with $T = 1$ s and the beginning of the following third and the last part of test no. SAND-3 with $T = 0.5$ s (Fig. 11c), there is a certain difference ($\Delta S = 0.0015 - 0.0020$) in saturation conditions which in fact should not exist or, at least, should be much more smaller. At the moment it is rather difficult to give a reasonable explanation for this finding. Analysing only the part of experiment with $T = 0.5$ s, a further improvement of saturation conditions in the upper part of the sand model was found ($\Delta S = 0.0006$ in point Pt. 2).

Disregarding the results from test no. SAND-2, highly saturated soil conditions were indicated in all investigated cases.

4. CONCLUSIONS

The problem of the dynamic behaviour of the submarine pipeline buried in sandy seabed sediments was investigated numerically and experimentally. The numerical analysis has shown evidently the importance of the combined compressibility of the two-phase (*i.e.*, pore-fluid and soil skeleton) seabed medium on the hydrodynamic uplift force, comparable with the buoyancy force, acting on the pipeline.

A high value of the optimum degree of saturation, influencing directly the pore-fluid compressibility, is very likely to be found 'in-situ', especially in coastal and tidal regions.

On the other hand, one has to remember that it is extremely difficult, or even impossible, to measure exactly the degree of saturation under real and also laboratory conditions. Therefore, the small-scale laboratory experiments, with the pipeline buried and firmly fixed in the seabed model, were performed in order to verify the numerical analysis and to get a better knowledge on the influence of soil saturation conditions on the quantitative picture of the pore-pressure field in the pipeline vicinity. The comparison of the numerical results with the pore-pressure measurements in 5 points on the pipeline circumference has confirmed the existence of near-saturated soil conditions characterized by a relatively high value of the degree of saturation ($S > 0.992$).

The question of laboratory modelling of the dynamic behaviour of a free-movable pipeline buried in seabed sedimens will be undertaken and reported in due course.

ACKNOWLEDGEMENT

This work is a result of a joint research between the Department of Environmental and Civil Engineering, Okayama University, and the Marine Civil Engineering Department, Technical University og Gdańsk, in the period of October-November 1996. The Authors gratefully acknowledge the financial support provided by the WESCO Civil Engineering Company, Okayama, Japan. A part of this research was supported by the Scientific Research Program (Grant No. 08650609), Head researcher: Dr. Shiro Maeno) of the Ministry of Education, Science, Sports and Culture, Japan.

LITERATURE

Bobby, W., Arockiasamy, M., Haldar, A.K. (1979). Finite element analysis of pipe-soil-wave interaction. *Proc. of the 2nd International Conference on Off-shore Structures*, London, England, 28-31 August 1979, Paper No. 39, pp. 503-506.

Cheng, A.H.D., Liu, P.L.-F. (1986). Seepage force on a pipeline buried in a poro-elastic seabed under wave loading. *Applied Ocean Research*, 8(1), pp. 22-32.

Lai, N.W., Dominguez, R.F., Dunlap, W.A. (1974). Numerical solutions for determining wave-induced pressure distributions around buried pipelines. Texas A & M University, Sea Grant Pub. No. TAMU-SG-75-205.

Lennon, G.P. (1983). Wave-induced forces on buried pipelines. *Proc. of the Coastal Structures '83*, Arlington, pp. 505-518.

Lennon, G.P. (1985). Wave-induced forces on buried pipelines. *Journal of Waterway, Port, Coastal and Ocean Engineering*, ASCE, 111(3), pp. 511-524.

Liu, P.L.F., O'Donnel, T.P. (1979). Wave-induced forces on buried pipelines in permeable seabed. *Journal of Waterway, Port, Coastal and Ocean Division*, Vol. 104, No. WW4.

MacPherson, H. (1978). Wave forces on pipeline buried in permeable seabed. *Journal of Waterway, Port, Coastal and Ocean Division*, ASCE, 104(WW4), pp. 407-419.

Madsen, O.S. (1978). Wave-induced pore pressures and effective stresses in a porous bed. *Gèotechnique*, 28(4), pp. 377-393.

Maeno, S., Nago, H. (1988). Settlement of a concrete block into a sand bed under water pressure variation *Proc. of the Conference on Modelling Soil-Water-Structure Interaction (SOWAS '88)*, Kolkman *et al.* (eds), Balkema, Rotterdam, pp. 67-76.

Maeno, S., Nago, H. (1991). Numerical analysis on the dynamic behaviour of sea bed around breakwater. *Proc. of the Conference GEO-COAST '91*, Yokohama, 3-6 Sept. 1991, pp. 591-596.

Maeno, S., Yamamoto, T., Nago, H. (1996). Numerical analysis of dynamic behaviour of highly saturated sand bed around cylindrical block under cyclic loading of water pressure. *Journal of The Faculty of Environmental Science and Technology, Okayama University*, Vol. 1, No. 1, pp. 121-133.

Magda, W. (1992[a]). *Wave-Induced Pore-Pressure Distribution In Sandy Seabed Sediments.* Ph.D. Thesis, Technical University of Gdansk, Gdansk, Poland.

Magda, W. (1992[b]). Wave-induced pore water pressure acting on a buried submarine pipeline. *Proc. of the 23rd International Conference on Coastal Engineering (ICCE'92)*, Venice, Italy, 4-9 October 1992, pp. 3135-3148.

Magda, W. (1994). Analytical solution for the wave-induced excess pore-pressure in a finite-thickness seabed layer. *Proc. of the 24th International Conference on Coastal Engineering (ICCE '94)*, 23-28 October 1994, Kobe, Japan, pp. 3111-3125.

Magda, W. (1995). Wave-induced uplift force acting on a buried submarine pipeline - a practical engineering approach. *Proc. of the International Conference on Coastal and Port Engineering in Developing Countries (COPEDEC '95)*, 25-29 September 1995, Rio de Janeiro, Brazil, pp. 2295-2310.

Magda, W. (1996). Wave-induced uplift force acting on a submarine buried pipeline. Finite element formulation and verification of computations. *Computers and Geotechnics*, 19(1), pp. 47-73.

Magda, W. (1997). Wave-induced uplift force on a submarine pipeline buried in a compressible seabed. *Ocean Engineering*, Vol. 24, No. 6, pp. 551-576.

McDougal, W.G., Davidson, S.H., Monkmeyer, P.L., Sollit, C.K. (1988). Wave-induced forces on buried pipelines. *Journal of Waterway, Port, Coastal and Ocean Engineering*, ASCE, 114(2), pp. 220-236.

Monkmeyer, P.L., Mantovani, P., Vincent, H. (1983). Wave-induced seepage effects on a buried pipeline. *Proc. of the Coastal Structures '83 Conference*, pp. 519-531.

Nago, H. (1981). Liquefaction of highly saturated sand layer under oscillating water pressure. *Memoirs of the School of Engineering*, Okayama University, Vol. 16, No. 1, pp. 93-104.

Nago, H., Maeno, S. (1984). Pore water pressure in sand bed under oscillating water pressure. *Memoirs of the School of Engineering, Okayama University*, Vol. 19, No. 1, pp. 13-32.

Nago, H., Maeno, S. (1986[a]). Dynamic behaviour of sand bed under oscillating water pressure. *Memoirs of the School of Engineering*, Okayama University, Vol. 20, No. 2, pp. 81-91.

Nago, H., Maeno, S. (1986[b]). Dynamic behaviour of sand bed around structure under wave motion. *Memoirs of the School of Engineering*, Okayama University, Vol. 21, No. 1, pp. 81-91.

Nago, H., Maeno, S. (1987). Pore pressure and effective stress in a highly saturated sand bed under water pressure variation on its surface. *Natural Disaster Science*, 9(1), pp. 23-35.

Okusa, S. (1985). Wave-induced stresses in unsaturated submarine sediments. *Gèotechnique*, 35(4), pp. 517-532.

Phillips, B.A., Ghazzaly, O.I., Kalajian, E.H. (1979). Stability of pipeline in sand under wave pressure. *Proc. of the Speciality Conference 'Civil Engineering in the Ocean IV'*, San Francisco, pp. 122-136.

Verruijt, A. (1969). Elastic storage of aquifers. In: *Flow Through Porous Media*. de Wiest (ed.), Academic Press, New York and London, pp. 331-376.

Yamamoto, T., Koning, H.L., Sellmeijer, H., Hijum, E. (1978). On the response of a poro-elastic bed to water waves. *Journal of Fluid Mechanics*, ASCE, 87, pp. 193-206.